analytical chemistry

Article

pubs.acs.org/ac

Relative Quantification of Phospholipids Based on Isotope-Labeled Methylation by Nanoflow Ultrahigh Performance Liquid Chromatography−Tandem Mass Spectrometry: Enhancement in Cardiolipin Profiling

Jong Cheol Lee, Seul Kee Byeon, and Myeong Hee Moon*

Department of Chemistry, Yonsei University, 50 Yonsei-ro, Seodaemun-gu, Seoul 03722, Korea

Supporting Information

ABSTRACT: In this study, lipid analysis based on isotope-labeled methlylation (ILM) was performed by nanoflow ultrahigh performance liquid chromatography−eletrospray ionization-tandem mass spectrometry (nUPLC−ESI-MS/MS) for enhanced detection and quantification of targeted phospholipids. ILM depends on methylation of phosphate groups by (trimethylsilyl)diazomethane, and the ILM based quantitation with reversed phase nUPLC−ESI-MS/MS provides advantages in PL profiling such as enhanced detectability of methylated PLs owing to increased hydrophobicity and substantial increase in resolution due to the increase of retention. Efficacy of ILM in nUPLC−ESI-MS/MS analysis was evaluated in the selected reaction monitoring (SRM) method by varying the mixing ratio of H-/D-methylated PL standards, which resulted in the successful quantification of 24 species, including phosphatidic acid (PA), phosphatidylserine (PS), phosphatidylglycerol (PG), ceramide-1-phosphate (Cer1P), phosphoinositides, and cardiolipin (CL), with ∼6.6% variation in the calculated ratio of H-/D-methylated PLs. The method was applied to the lipid extracts from a DU145 cell line after D-allose treatment, resulting in the quantification of 83 PLs of which results were not statistically different from those obtained by conventional quantification methods. Morever, detection and quantification of CLs and PAs were evidenced to be highly effective when used with the ILM method as 43 CLs and 20 PAs from cellular lipid extracts were analyzed while only 18 CLs and 12 PAs were identified when conventional methods were carried out. This proves the ILM combined with LC−MS to be a promising method for analysis of the aforementioned classes of lipids. Overall, the study highlighted the applicability of targeted quantification by the ILM method in lipidomic analysis and demonstrated an improvement in the detection of less abundant anionic PLs.

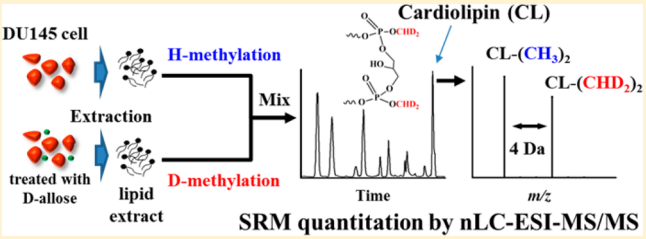

Lipids are major constituents of the cellular membrane and known to play critical roles in energy storage, intercellular signaling, cell proliferation, and apoptosis.[1,2] A number of studies have correlated perturbed lipid profiles with the progression of a variety of metabolic disorders such as diabetes, obesity, cardiovascular diseases, cancers, and rare diseases.[3−8] Owing to this, lipidomic analysis gains significant interest in understanding the role of lipids in the pathogenesis of these disorders as well as developing potential biomarkers from altered lipid species. Phospholipids (PLs) are the most abundant class of lipids characterized by different head groups as well as lengths and degrees of unsaturation of fatty acyl chains, and their analysis have been facilitated by employing tandem mass spectrometry (MS^n) which provides accurate determination of the molecular structures of lipids from fragment ion spectra. However, chromatographic separation of lipids is yet required prior to MS analysis owing to the complexity in their molecular structures, which minimizes possible ion suppression of the less abundant species as compared to that of the highly abundant ones. This is achieved via liquid chromatography (LC) coupled with electrospray ionization (ESI) MS^n (LC−ESI-MS^n).[9−11] In particular, incorporation of ultrahigh performance/pressure LC (UPLC), which utilizes a capillary LC column for lipid separation, offers several advantages, such as minimal sample size (few micrograms), enhanced resolution, and speed of separation. Recently, nanoflow LC coupled with MS (nLC−ESI-MS^n) has been applied for the qualitative and quantitative analysis of lipidome from plasma, urine, cells, and tissue samples in various diseases or other physiological conditions.[8,12−16]

When LC−MS or direct infusion method by MS alone is utilized for quantitative analysis, a set of internal standards specific to each class of lipid is added to the sample of interest, in order to compensate for the fluctuation in MS intensity across the runs as the analysis of samples is performed separately. Since the MS intensity of a particular PL molecule depends on the length of its acyl chain and the degree of unsaturation,[17] it is difficult to determine its accurate

Received: January 24, 2017
Accepted: April 11, 2017
Published: April 11, 2017

ACS Publications © 2017 American Chemical Society

DOI: 10.1021/acs.analchem.7b00297
Anal. Chem. 2017, 89, 4969−4977

concentration unless the molecular structure of an internal standard exactly matches with that of the target molecule.[18] Although the effects of unsaturation and length of acyl chains on the variation in MS intensity can be minimized at a low amount (less than ~1 pmol of PL molecule) with the use of nLC−ESI-MS^n,[19] high-speed relative quantification of lipids is still a problem. To tackle this, a few isotope-labeled derivatization methods for PLs have been employed recently, which rely on the formation of tags in the primary amine, such as *N*-methylpiperazine amide,[20] 4-(dimethylamino) benzoic acid (DMABA),[21] *S*,*S*′-dimethylthiobutanoyl hydroxysuccinimide (DMBNHS),[22] and isopropyl moieties.[23] These methods, however, are limited to PLs containing amine groups, such as PE and PS. Methylation of phosphate in PLs with either (trimethylsilyl)diazomethane (TMSD) or ^{13}C-diazomethane was reported to increase the sensitivity of MS detection.[24−27] Methylation coupled with isotope labeling has shown to facilitate the relative quantification of phosphoinositides (PIP) as well as a number of other PLs.[28,29] These studies, however, were carried out mostly with direct infusion to ESI-MS/MS except a study using supercritical fluid chromatography (SFC) with tandem MS[24] and another study analyzing phosphoinositides using LC−ESI-MS/MS,[25] but the dynamic application of a methylation method for the relative quantification of a wide range of PLs with LC−ESI-MS^n was not examined in detail.

In this study, lipid analysis using the isotope-labeled methylation (ILM) method was applied to nUPLC−ESI-MS^n and its optimized setting including mobile phases and ionization modifier was established through various evaluations. The method was validated by the global identification and quantification of PLs in cells, using TMSD shown in Scheme 1.

Scheme 1. Isotope-Labeled Methylation (ILM) Method for Identification and Quantification of PLs Using TMSD

The detailed reaction mechanism is in scheme S1 of the Supporting Information. In the present study, systematic assessment in the efficiency of methylation of PLs was carried out by nUPLC−ESI-MS^n with the selected reaction monitoring (SRM) method, using PL standards (phosphatidylglycerol (PG), lysoPG (LPG), phosphatidylinositol (PI), lysoPI (LPI), phosphatidylserine (PS), lysoPS (LPS), phosphatidic acid (PA), lysoPA (LPA), and cardiolipin (CL)) by varying the mixing ratio (H/D) of H-labeled (−CH_3) and D-labeled (−CHD_2) methylation. Further, the effect of ionization modifiers on the detection of methylated PLs in the positive ion mode was examined. This method was applied to lipid extracts from hormone-refractory prostate cancer (HRPC) cell line (DU145), after treatment with D-allose, which is a naturally occurring monosaccharide and is known to inhibit proliferation of various cancer cell lines by reducing the levels of reactive oxygen species (ROS) in neutrophils.[30,31] This study demonstrated that ILM coupled with nUPLC−ESI-MS^n can serve as a powerful tool to quantify relative changes in PL profiles of the D-allose treated prostate cancer cells. The study also focused on the high-speed quantification with enhanced detection of PS and CL, which are closely associated with apoptosis.[32] ILM-based quantification of PLs from cancer cells was compared with the individual quantifications which utilize addition of internal standards to samples for analysis.

EXPERIMENTAL SECTION

Materials and Reagents. The PL standards, HPLC grade solvents, ionization modifiers, and other reagents are listed in the Supporting Information.

Cell Culture and Lipid Extraction. The DU145 HRPC cell lines were procured from the Korean Cell Line Bank (Seoul, Korea). Cells were cultured in RPMI 1640 medium (Invitrogen, Carlsbad, CA) added with 10% heat inactivated fetal bovine serum (FBS) and 1% penicillin/streptomycin in a 100 mm Petri dish, followed by incubation in a 37 °C incubator in humidified atmosphere with 5% CO_2 for 48−72 h. For D-allose treatment, 40 mM D-allose was added to the culture medium. When the cells occupied more than 90% of dish area, they were detached by the addition of 0.25% trypsin-EDTA. This led to collection of approximately 6×10^6 cells/mL.

Extraction of lipids was performed according to the Folch method modified with MTBE/CH_3OH.[33] Briefly, the collected cell pellets were vacuum-dried, followed by the addition of MeOH (300 μL). The samples were sonicated for 1 min for homogenization. Thereafter, 1 mL of MTBE was added to the homogenate and the samples were vortexed for 1 h. Following this, 250 μL of 2.05 M HCl was added to the mixture. The samples were vortexed for 10 min, followed by centrifugation at 1000*g* for 10 min. The upper organic layer was transferred to a new tube, and the remaining lower layer was re-extracted using 400 μL of organic (upper) layer of MTBE/MeOH/H_2O (10:3:2.5, v/v/v) mixture, followed by vortexing for 10 min and centrifugation at 1000*g* for 5 min. The upper layer was pooled with the previously collected organic layer. The combined organic layers were washed with 500 μL of aqueous (lower) layer of the above solvent mixture (MTBE/MeOH/H_2O) by vortexing for 10 min, followed by centrifugation at 1000*g* for 5 min. The final organic layer was transferred to another tube for derivatization.

Isotope-Labeled Methylation (ILM). Methylation of phosphate group of PLs began by the addition of 50 μL of CH_3OH and 50 μL of TMSD (2 M in hexane, yellow color) to PL standard mixtures or the organic layer of cell extracts, followed by vortexing the mixture for 10 min at room temperature. To quench the reaction, 6 μL of glacial acetic acid was added to the mixture, following which the yellowish solution turned transparent. To this mixture, 500 μL of aqueous (lower) layer of the fresh solvent mixture of MTBE/CH_3OH/H_2O (10:3:2.5, v/v/v) was added for washing. The mixture was vortexed for 10 min and centrifuged at 1000*g* for 5 min. The final organic layer was vacuum-dried and dissolved in 200 μL of $CH_3OH/CHCl_3$ (9:1, v/v) for storage. This mixture was diluted with CH_3OH/H_2O (8:2, v/v) for nUPLC−ESI-MS/MS analysis. ILM was achieved by replacing CH_3OH, H_2O, and HCl with CD_3OD, D_2O, and DCl, respectively, during all extraction and derivatization procedures.

nUPLC−ESI-MS^n Analysis. Two nUPLC−ESI-MS/MS systems were used in the present study. Nontargeted lipid identification was accomplished with a Dionex Ultimate 3000 RSLCnano System with autosampler equipped with LTQ Velos ion trap mass spectrometer from Thermo Scientific (San Jose, CA). SRM quantitation of lipids was carried out using a nanoACQUITY UPLC system from Waters coupled to a TSQ Vantage triple-stage quadrupole MS system from Thermo Scientific. Analytical columns are prepared in the laboratory,

DOI: 10.1021/acs.analchem.7b00297
Anal. Chem. 2017, 89, 4969−4977

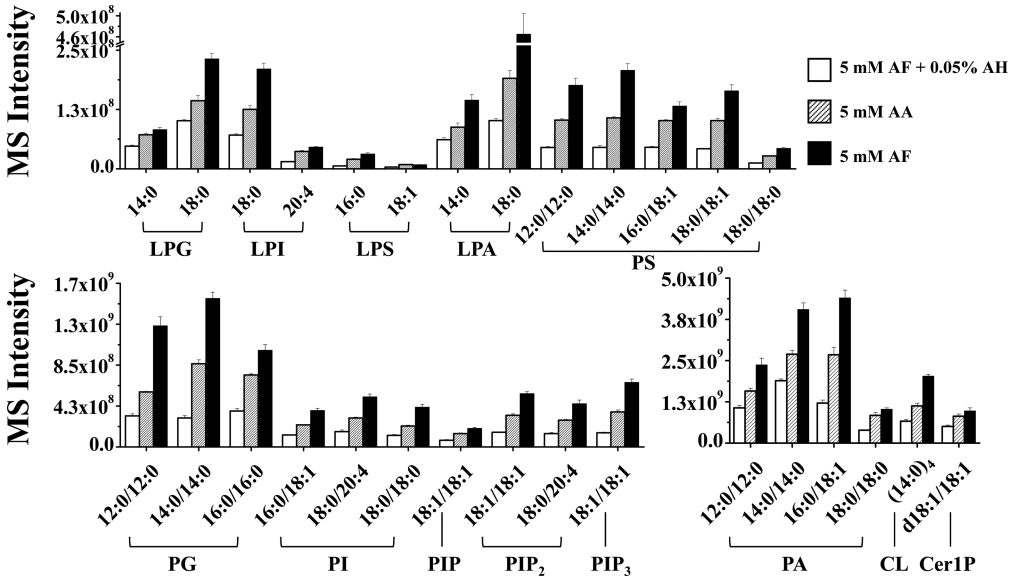

Figure 1. Effect of ionization modifiers of mobile phase on the ionization efficiencies of 29 methylated PL standards of different categories in positive ion mode by nUPLC–ESI-MS/MS.

and the details of column preparations with the system configuration are in the Supporting Information. Mobile phase used for lipid separation was (9.5:0.5, v/v) H_2O/CH_3CN for A and (2:2:6, v/v/v) MeOH/CH_3CN/IPA for B, added with 0.05% ammonium hydroxide (AH) as ionization modifier in negative ion mode and 5 mM ammonium formate (AF) in positive ion mode.

For the nontargeted analysis of lipids from cells, 10 μg (2 μL, 5 μg/μL) of the lipid extract was loaded to an analytical column with mobile phase A at 700 nL/min for 10 min, with the switching valve off. After injection, the switching valve was turned on, the pump flow rate was set to 7 μL/min, and the resulting column flow rate was adjusted to 300 nL/min. Gradient elution-I (the run condition I) began by ramping the mobile phase B from 0 to 60% for 0.1 min, to 75% for 5 min, to 80% for 10 min, to 90% for 10 min, and further to 99% for 5 min. At 99%, the mobile phase B was maintained for 20 min to wash the column and was then resumed to 0% for 10 min for re-equilibrating the column. The ESI voltage for the ion trap MS was set to 3.0 kV. The m/z range of the precursor scan MS was 400–1600, and data-dependent CID analyses was accomplished at 40% normalized collision energy. Molecular structures of lipids were determined by LiPilot software, an algorithm based on fragment ion spectra of lipid molecules, developed in our laboratory[34] and confirmed by manual examinations.

SRM-based quantification of methylated lipids was performed under different run conditions. Lipid extracts from DU145 cell line were treated with H-labeled methylation, and extracts from D-allose-treated cells were treated with D-labeled methylation. The methylated lipid samples were mixed at a 1:1 (H/D) ratio (10 μg/μL for each lipid sample) and were subjected to nUPLC–ESI-MS/MS analysis. The lipid mixture (2 μL, 10 μg) was loaded to the same analytical column used for the nontargeted identification, using mobile phase A at a flow rate of 700 nL/min for 10 min. After sample loading, the pump flow rate was ramped to 14 μL/min with the switching valve on, so that the column flow rate could be adjusted to 300 nL/min. Gradient elution-II began by increasing the mobile phase B to 70% for 0.1 min, to 80% for 5 min, and finally to 100% for 10 min. Thereafter, it was maintained at 100% for 10 min for washing the column and resumed to 0% for 5 min. Detection of methylated PLs was performed in the positive ion mode at 3.0 kV of ESI with a scan width of m/z 1.0 and scan time of 0.001 s. SRM quantification of methylated lipids was carried out at 25 V of CID for all the classes. In the case of CL species having a m/z value >1500, SRM quantification was carried out using ion trap MS. To validate the results obtained in the ILM method, conventional quantification experiments were carried out by analyzing individual lipid extracts (0.5 pmol/μL) along with a set of internal standards having odd-numbered acyl chains. The relative change in each individual lipid molecule was analyzed by calculating the ratio of corrected peak area (relative to the peak area of each standard) of the two samples.

RESULTS AND DISCUSSION

nUPLC–ESI-MS^n Analysis of Methylated PLs. Methylation was performed for a mixture of PL standards with different head groups: PG, PI, PS, PA, PIP$_n$ (PIP molecules with different degrees of phosphorylation at inositol group), CL, and Cer1P. Methylation of phosphate groups leads to increased hydrophobicity of PL which improves ionization efficiency, since hydrophobic molecules tend to be separated easily from other interfering compounds during ESI with a tendency of staying on the surface of the droplet, which would result in increased ionization efficiency. Moreover, an increase in hydrophobicity causes a longer retention in a reversed phase column, resulting in the case of a substance eluting at a condition with a higher proportion of organic solvent, which is more advantageous to generate charged droplets.[35] Therefore, the effect of ionization modifier added to mobile phase of LC needed to be examined. In this experiment, three ionization modifiers were tested with 29 PL standards post H-methylation by comparing their MS intensities. The effect of ionization modifiers, including a mixed modifier (5 mM AF + 0.05% AH) that has been utilized as a universal modifier for both positive and negative ion modes, 5 mM ammonium acetate (AA) utilized for the MS analysis of the methylated phosphoinosi-

DOI: 10.1021/acs.analchem.7b00297
Anal. Chem. 2017, 89, 4969–4977

tides,[28] and 5 mM AF, on MS intensities of methylated PLs is shown in Figure 1. Most of the PLs were detected in their protonated forms ($[M + H]^+$). However, PG, PI, PA, and CLs were predominately detected as ammonium adduct ions ($[M + NH_4]^+$). They were detected in the protonated forms, $[M + H]^+$ as well but as illustrated in Figure S1, they can be considered negligible. As can be seen in Figure 1, 5 mM AF provided the highest (up to ~2-fold) ionization intensities for all the PL groups including PIP_n molecules. Therefore, 5 mM AF was used as the ionization modifier in mobile phase solutions for further analysis.

Increased hydrophobicity of PLs upon methylation resulted in an increase in the retention time and, more specifically, the ionization efficiency of polar PLs. Figure 2 demonstrates the

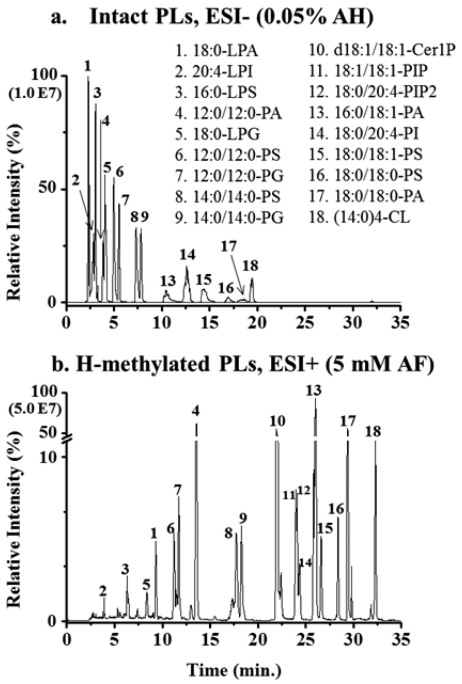

Figure 2. Base peak chromatograms of (a) intact PL standards in negative ion mode and (b) H-methylated PL standards in positive ion mode of nUPLC−ESI-MS/MS. Mobile phase solutions are the same for both runs except the ionization modifier (0.05% AH for part a and 5 mM AF for part b).

extracted ion chromatograms (EICs) of (a) 18 intact PL standard mixtures (1 pmol each) obtained in negative ion mode with 0.05% AH added to mobile phases and (b) H-methylated PL standards in positive ion mode with 5 mM AF obtained by nUPLC−ESI-MS/MS. The chromatogram in Figure 2b was obtained with a 1:1 mixture of H-methylated and D-methylated PL standards (1 pmol each). Methylation of PLs resulted in an increase in retention time (Figure 2b). The widths for the peak nos. 13−18, however, were significantly reduced with an increase in intensity: 0.25 min for intact vs 0.09 min for H-methylated $(14:0)_4$-CL (peak no. 18) based on the peak width at half the height. Since the degree of methylation varied with the number of polar head groups on PLs (1 for PI and PG, 2 for PS, PA, and CL, 3 for PIP, 5 for PIP_2, and 7 for PIP_3), extended retention times were obtained for the molecules having higher degree of methylation (peak nos. 1, 4, 6, 8, and 18) as compared to the intact molecules (Table S1 of the Supporting Information). Moreover, PIP_n molecules, under their intact conditions, were not detected successfully in the negative ion mode of MS owing to the presence of additional phosphate groups in inositol (Figure 2a). The methylation of the terminal phosphate groups, however, enhanced the detection efficiency of peak nos. 11 and 12 owing to the increased hydrophobicity. Additionally, Cer1P (no. 10) and PA (nos. 13 and 17) molecules also exhibited increased MS intensity upon methylation. It should be noted here that methylation followed by a significant increase in the retention time was successfully achieved for cardiolipin (CL) (peak no. 18), leading to its enhanced detection. Analysis of CL by reversed phase LC (RPLC) with MS has been relatively difficult owing to the prolonged retention due to the presence of four acyl chains in the CL molecule as well as poor ionization during ESI because of two phosphate groups. Methylation had a great potential for the selective profiling of low-abundance CLs specifically found in mitochondria. Since mitochondrial dysfunction is a prelude to neurodegenerative disorders,[36] efficient analysis of CLs may prove to be extremely useful for the assessment of involvement of lipids in mitochondria-associated diseases. The enhancement of CL profiling from cellular extracts will be discussed later in detail.

To examine the differences in retention of the H- and D-methylated PL pairs, the retention times of each pair of methylated PLs were compared with each other. The base peak chromatogram of a 1:1 mixture of the H-and D-methylated PL standards is shown in Figure S2. The average retention times ($n = 3$) of each H- and D-methylated species together with the relative differences in retention times of each pair is listed in Table S1. Both the H- and D-methylated species eluted nearly at the same time with the maximum difference of less than 0.09 min for the 18 species. This suggests that the light and heavy labeled PLs exhibit relatively similar retention times during nUPLC separation.

The molecular structures of H- and D-methylated PLs can be distinguished based on the differences in their precursor ion m/z values, along with the data-dependent CID fragment ion spectra obtained by MS/MS/MS (MS^3). The spectra of H- and D-methylated PL molecules obtained by nUPLC−ESI-MS^n analysis is shown in Figure 3: (a) precursor ion MS spectrum of the peak number 13 (16:0/18:1-PA at t_r = 26.05 min in Figure 2b) showing detection of the two labeled ions in the form of ammonium adduct at m/z 720.5 ($[M_H + NH_4]^+$, subscript H for H-methylation) and m/z 724.5 ($[M_D + NH_4]^+$, subscript D for D-methylation) with 4 Da difference due to the addition of two methyl groups and (b,c) their respective MS/MS spectra representing the loss of NH_3 at m/z 703.6 ($[M_H + NH_4 - NH_3]^+$) and m/z 707.7 ($[M_D + NH_4 - NH_3]^+$) together with the formation of a prominent and common fragment ion having the same m/z 577.5 as $[M_H - PO_2(OCH_3)_2]^+$ and $[M_D - PO_2(OCHD_2)_2]^+$. Figure 3d shows the MS^3 spectra of the common ion m/z 577.5 in run b, representing the loss of acyl chain in the form of carboxylic acid at m/z 321.4 ($[M_H - PO_2(OCH_3)_2 - R_1COOH]^+$) and m/z 295.4 ($[M_H - PO_2(OCH_3)_2 - R_2COOH]^+$), acylium ions ($[RCO]^+$) at m/z 239.3 and 265.3, and the loss of water ($[RCO - H_2O]^+$) from acylium ion at m/z 211.3 and 247.3. On the basis of the CID spectra with the characteristic fragment ions, they can be easily identified as H-methylated and D-methylated 16:0/18:1-PA molecules.

In addition to the methylation that was expected to occur, overmethylation in the free hydroxyl group of the headgroup of PLs may take place. When 14:0/14:0-PG is overmethylated, its

DOI: 10.1021/acs.analchem.7b00297
Anal. Chem. 2017, 89, 4969−4977

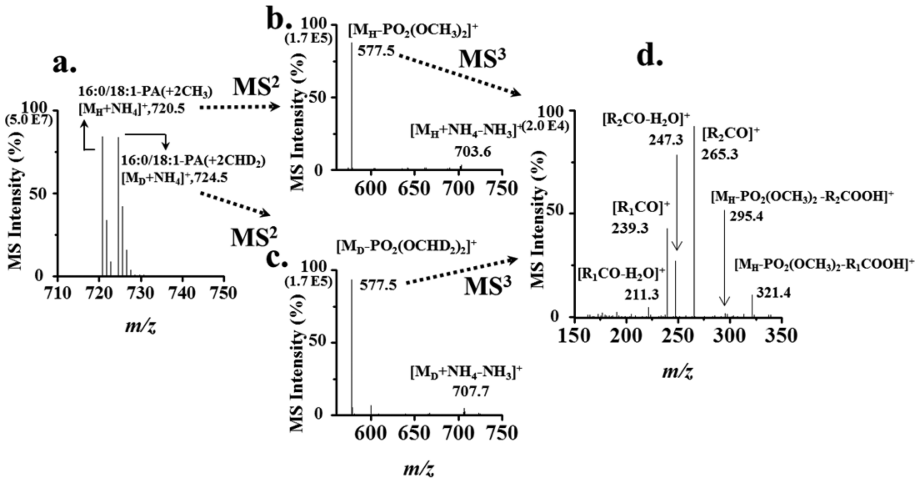

Figure 3. (a) Precursor MS scan at t_r = 26.05 min representing H- and D-methylated pair of 16:0/18:1-PA (peak no. 13 in Figure 2b), (b) CID (MS^2) spectra of the parent ion m/z 720.5 (two H-methylation), (c) CID (MS^2) spectra of the parent ion m/z 724.5 (two D-methylation), and (d) MS^3 spectra of the product ion m/z 577.5 from both runs showing the identical CID spectra representing the typical fragments supporting the acyl chain structures obtained by nUPLC−ESI-MS^3.

Table 1. Effect of Acid Treatment on Methylation of PLs with TMSD[a]

		methylation efficiency (%)			
class	acyl chain	normal	RSD (%)	acid	RSD (%)
LPG	14:0	84.59 ± 5.33	6.30	84.59 ± 5.33	5.72
PG	18:0	91.29 ± 10.17	11.14	91.29 ± 10.17	10.76
	12:0/12:0	91.10 ± 7.51	8.25	91.10 ± 7.51	7.86
LPI	14:0/14:0	85.68 ± 7.42	8.66	85.68 ± 7.42	7.95
	16:0/16:0	79.08 ± 2.21	2.79	79.08 ± 2.21	2.16
	18:0	90.99 ± 10.47	11.51	90.99 ± 10.47	11.42
PI	20:4	89.24 ± 6.04	6.77	89.24 ± 6.04	6.62
	16:0/18:1	90.21 ± 2.12	2.35	90.21 ± 2.12	2.09
LPS	18:0/18:0	94.13 ± 10.52	11.18	94.13 ± 10.52	10.93
	18:0/20:4	92.46 ± 3.51	3.79	92.46 ± 3.51	3.63
	16:0	89.91 ± 5.22	5.81	89.91 ± 5.22	5.54
PS	18:1	83.07 ± 8.61	10.36	83.07 ± 8.61	9.32
	12:0/12:0	85.96 ± 6.70	7.79	85.96 ± 6.70	7.14
LPA	14:0/14:0	79.61 ± 7.75	9.74	79.61 ± 7.75	8.47
	16:0/18:1	75.45 ± 6.54	8.66	75.45 ± 6.54	7.10
	18:0/18:1	77.69 ± 3.79	4.88	77.69 ± 3.79	3.70
	18:0/18:0	83.21 ± 7.98	9.60	83.21 ± 7.98	8.52
	14:0	80.84 ± 5.65	6.99	80.84 ± 5.65	6.08
PA	18:0	76.82 ± 6.17	8.03	76.82 ± 6.17	6.53
	12:0/12:0	86.15 ± 4.97	5.77	86.15 ± 4.97	5.18
CL	14:0/14:0	90.90 ± 3.63	3.99	90.90 ± 3.63	3.68
	16:0/18:1	93.87 ± 5.09	5.42	93.87 ± 5.09	5.24
	18:0/18:0	91.38 ± 10.81	11.83	91.38 ± 10.81	11.31
	$(14:0)_4$	86.68 ± 8.81	10.16	86.68 ± 8.81	9.40

[a]Methylation efficiency is based on the relative amount of methylated species, which was calculated by subtracting the peak area of intact PL molecules in methylated sample mixtures from that of the same PL molecule without undergoing a methylation reaction.

m/z value increases by 14 Da (1OM = 1 overmethylation) to 712.5, which results in additional peaks at t_r = 18.80 and 19.23 min, which is shown in Figure S3b. With overmethylation, hydrophobicity increased and its retention time was shifted to larger scale. Since PG has two free hydroxyl groups in the headgroup, two different peaks can be observed by the separation of positional isomers of overmethylation. Despite the fact that overmethylation does take place, it does not significantly affect the relative quantitation since the amount of overmethylation is not significant (see the peak area difference between the peak a and the small peaks at 18.80 min of Figure S3b. Also, even if m/z of overmethylated lipid shares the same m/z of other D-methylated lipids and their MS^2 spectra might be the same (Figure S3e,f), the present LC separated these lipids as overmethaylated 14:0/14:0-PGs at 18.80 and 19.23 min while D-methylated 14:0/14:0-PS eluted at 17.66 min (Figure S3b). Overmethylation of Cer1P and CL with free hydroxyl groups were negligible as shown in Figure S4.

Efficiency of Methylation. The yield of methylation reaction increased under acidic conditions (pH = 1−2),

DOI: 10.1021/acs.analchem.7b00297
Anal. Chem. 2017, 89, 4969−4977

achieved by adding HCl. The methylation efficiencies (%) of 24 lipid standards with or without the addition of HCl have been compared in Table 1. The methylation efficiency represents the percentage of methylated species relative to initial intact PL species. The amount of methylated species was calculated by subtracting the peak area (relative to an internal standard of each specific PL class) of the precursor ion of nonmethylated species post methylation from that of the same molecule without methylation. Since the ionization efficiencies of the methylated and nonmethylated species during ESI were different from each other owing to the increased hydrophobicity of the methylated species, a comparison of peak area of the molecules was carried out based on the amount of intact PL molecules left after methylation in the negative ion mode of nUPLC−ESI-MS/MS. Table 1 indicates that efficiency of methylation of PLs under acidic conditions was above 96% for most of the classes except the LPI molecules (~92.4%), while 75−94% efficiency was obtained under neutral conditions which are rather headgroup specific. Efficiency data for Cer1P and PIP_n were not included in Table 1, since these molecules were not resolved by the reversed phase nUPLC−ESI-MS/MS. These molecules, however, were well detected post methylation. According to the literature, the methylation efficiencies of Cer1P and PIP_n were reported to be 93.8 ± 0.2% and close to complete, respectively.[24,28] While the methylation efficiency in this particular method was based on the calculation of the remaining intact PL molecules, it is not sure whether all the molecules underwent methylation. This was further investigated by measuring the relative ratio of H- and D-methylated standard mixtures by varying the mixing ratio later.

ILM-Based Quantification of PLs by nUPLC−ESI-MS/MS. ILM-based quantification by nUPLC−ESI-MS/MS analysis was performed for quantifying the 29 methylated PL standard pairs (H- and D-methylation). The H- and D-methylated PL standards were mixed at five different ratios, H/D of 0.25 (2:8), 0.67 (4:6), 1.00 (5:5), 1.50 (6:4), and 4.00 (8:2) and were quantified by nUPLC−ESI-MS/MS according to the selected reaction monitoring (SRM) method. For SRM quantitation, the type of quantifier ion for each PL class was selected from the first MS/MS spectra of a standard species in each lipid class (Table S2 of the Supporting Information). Figure 4a represents the correlation between the calculated peak area ratio (H/D) of H-/D-methylated 16:0/18:1-PS and the mixing ratio obtained by nUPLC−ESI-MS/MS, indicating a good linear relationship between 0.25 to 4.00 of H/D. Figure 4b shows the superimposed extracted ion chromatograms (EICs) of H- and D-methylated PS molecules (triplicate measurements of each sample) with an average H/D value of 4.19 ± 0.17, which deviated about 5% from the mixed ratio (4.00). The retention times of each species were 14.96 ± 0.04 for both the H- and D-methylated PS, and the variations were negligible. The ratio of calculated peak area (H/D) of the 24 methylated PL species are listed in Table 2. While PLs from most of the classes displayed reasonable H/D ratio in the experiments compared to the mixing ratio within 6.6% of relative variation on average, only PI, including LPI, exhibited significant deviations of average 42.6% in the experimental H/D ratio from the expected value. This discrepancy may have originated from the steric hindrance caused by the cyclic ring of the inositol headgroup, which is relatively large compared to other head groups of PLs. This shows that methylation of PI molecules is not as efficient as other PL molecules. However, PIP molecules having different degrees of phosphorylation displayed good correlations (within 6.14% error on average in Table 2) with the expected H/D values. In PIP, PIP_2, and PIP_3, methylation at phosphate group at the glycerol backbone and methylation of the terminal phosphates at inositol headgroup (2 methylations per terminal phosphate) were performed successfully.

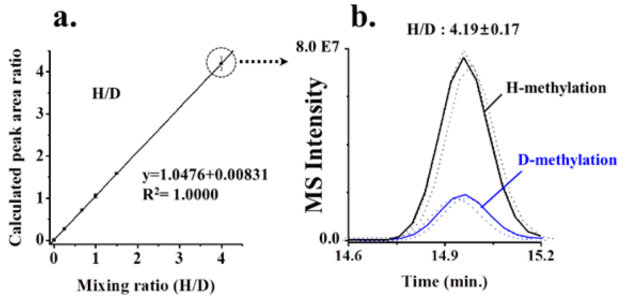

Figure 4. (a) Linear relationship between peak area ratio and various mixing ratios (H/D) of methylated 16:0/18:1-PS obtained by nUPLC−ESI-MS/MS and (b) extracted ion chromatograms (EICs) of H-methylated and D-methylated PS molecules from the three repeated runs at a mixing ratio (H/D) of 4, which yielded with experimental H/D ratio of 4.19 ± 0.17.

Effect of matrix on the methylation-based quantification was evaluated by adding odd-numbered acyl chain PL standards to the cellular lipid extracts from DU145 cells, followed by treatment of equal aliquots of mixtures for H- and D-methylation. Each of H- and D-methylated PL standards contained in the cellular lipid extracts were mixed in the same way by varying the mixing ratios (0.25, 0.67, 1.00, 1.50, and 4.00 of H/D). The resultant mixtures were analyzed as described above. The calculated ratio of H/D methylated species listed in Table S3 indicate that deviations from the expected ratio were less than average 6.3% for most of the species, nearly similar to the average deviation observed in Table 2. This implies that the effect of matrix from cellular extracts is not significant.

ILM-Based Quantification of PL Extracts of HRPC Cells by nUPLC−ESI-MS/MS. The ILM method was applied for the relative quantification of PLs extracted from HRPC DU145 cells with or without the treatment of D-allose. The PL extract from the D-allose treated cells were D-methylated and those from intact cells were H-methylated. Equal aliquots of both the methylated products were mixed together for nUPLC−ESI-MS/MS analysis (BPCs of the two samples in Figure S-5). ILM-based quantification of cellular PLs was carried out only for PG, PS, PA, and CL classes. Phosphatidylcholine (PC) and phosphatidylethanolamine (PE) were not included for ILM-based quantification since methylation at the primary amine group of PE produced PC molecules which can hardly be distinguished from original PC molecules in cellular extracts.

Structural analysis of these four PL classes identified a total of 112 species (1 LPG, 33 PGs, 1 LPS, 14 PSs, 2 LPAs, 18 PAs, and 43 CLs). Quantification was performed with 83 PLs because SRM does not distinguish between the isomeric structures of acyl chains, except for the PA molecules. The peak area ratios (D/H) calculated for PL species are listed in Table S4, along with the identified molecular structures of isomeric forms by CID experiments. Among the 112 species, 8 PAs and 25 CLs were exclusively identified from the methylated PLs, while these were not detected from intact PL extracts (marked as ∗ in Table S4) using the conventional method in negative

DOI: 10.1021/acs.analchem.7b00297
Anal. Chem. 2017, 89, 4969−4977

Table 2. Calculated Peak Area Ratio (H/D) of H- and D-Labeled Methylation PL Mixtures at Various Mixing Ratio (H/D) for Nine Different PL Classes

			calculated peak area ratio (H/D)									
class	no. of methyl groups	acyl chain	0.25 (2:8)[a]	RSD (%)	0.67 (4:6)[a]	RSD (%)	1.00 (5:5)[a]	RSD (%)	1.50 (6:4)[a]	RSD (%)	4.00 (8:2)[a]	RSD (%)
LPG	1	14:0	0.27 ± 0.01	3.96	0.72 ± 0.04	5.92	1.06 ± 0.04	3.49	1.59 ± 0.05	2.99	3.82 ± 0.18	4.61
		18:0	0.26 ± 0.01	4.22	0.69 ± 0.04	5.52	1.06 ± 0.09	8.61	1.56 ± 0.07	4.54	3.90 ± 0.25	6.34
PG	1	12:0/12:0	0.25 ± 0.01	4.86	0.71 ± 0.06	7.87	0.99 ± 0.09	8.95	1.45 ± 0.09	5.91	4.03 ± 0.31	7.70
		14:0/14:0	0.27 ± 0.02	7.12	0.70 ± 0.04	5.49	1.06 ± 0.06	5.39	1.59 ± 0.08	4.76	3.92 ± 0.16	4.05
		16:0/16:0	0.27 ± 0.02	7.85	0.66 ± 0.05	6.90	1.00 ± 0.03	3.15	1.47 ± 0.10	6.70	3.78 ± 0.25	6.60
LPS	2	16:0	0.27 ± 0.02	8.75	0.72 ± 0.04	5.46	1.06 ± 0.04	4.15	1.61 ± 0.19	11.47	4.24 ± 0.15	3.45
		18:1	0.24 ± 0.02	9.89	0.64 ± 0.04	5.99	1.07 ± 0.11	10.51	1.59 ± 0.15	9.70	4.18 ± 0.12	2.81
PS	2	12:0/12:0	0.26 ± 0.01	4.43	0.64 ± 0.01	1.79	1.00 ± 0.03	2.89	1.44 ± 0.02	1.16	3.85 ± 0.28	7.15
		14:0/14:0	0.27 ± 0.01	2.75	0.69 ± 0.03	4.04	0.99 ± 0.04	3.68	1.48 ± 0.02	1.05	3.89 ± 0.13	3.46
		16:0/18:1	0.27 ± 0.01	2.40	0.71 ± 0.02	3.29	1.05 ± 0.05	4.54	1.59 ± 0.02	1.19	4.19 ± 0.17	4.08
		18:0/18:1	0.26 ± 0.01	2.95	0.71 ± 0.02	2.46	1.06 ± 0.03	3.16	1.57 ± 0.01	0.54	4.21 ± 0.19	4.60
		18:0/18:0	0.27 ± 0.01	3.37	0.71 ± 0.03	4.02	1.06 ± 0.02	1.46	1.61 ± 0.08	5.05	4.19 ± 0.17	4.06
LPA	2	14:0	0.28 ± 0.01	3.68	0.71 ± 0.05	6.81	1.06 ± 0.07	6.79	1.57 ± 0.06	3.99	4.07 ± 0.35	8.54
		18:0	0.27 ± 0.02	6.29	0.70 ± 0.02	2.60	1.05 ± 0.05	4.72	1.59 ± 0.08	5.12	4.23 ± 0.16	3.80
PA	2	12:0/12:0	0.27 ± 0.01	3.33	0.69 ± 0.05	6.63	1.06 ± 0.08	7.92	1.58 ± 0.04	2.62	4.26 ± 0.20	4.73
		14:0/14:0	0.26 ± 0.02	6.65	0.70 ± 0.06	7.93	1.04 ± 0.02	2.38	1.59 ± 0.08	4.96	4.22 ± 0.30	7.02
		16:0/18:1	0.26 ± 0.01	4.26	0.71 ± 0.02	2.12	1.04 ± 0.03	3.00	1.61 ± 0.11	7.00	4.13 ± 0.15	3.71
		18:0/18:0	0.27 ± 0.01	3.39	0.70 ± 0.05	6.98	1.06 ± 0.03	2.68	1.60 ± 0.13	7.94	4.26 ± 0.16	3.75
PIP	3	18:1/18:1	0.26 ± 0.00	0.99	0.70 ± 0.01	2.10	1.06 ± 0.02	1.64	1.58 ± 0.05	2.88	4.21 ± 0.11	2.72
PIP_2	5	18:1/18:1	0.26 ± 0.01	2.75	0.71 ± 0.01	1.13	1.04 ± 0.01	0.65	1.57 ± 0.02	1.28	4.21 ± 0.06	1.47
		18:0/20:4	0.26 ± 0.00	1.66	0.70 ± 0.01	1.60	1.01 ± 0.01	0.84	1.58 ± 0.04	2.34	4.17 ± 0.10	2.39
PIP_3	7	18:1/18:1	0.28 ± 0.01	2.48	0.64 ± 0.01	1.04	0.91 ± 0.01	0.81	1.37 ± 0.05	3.90	3.65 ± 0.06	1.73
CL	2	$(14:0)_4$	0.27 ± 0.00	0.78	0.70 ± 0.00	0.59	1.05 ± 0.01	0.81	1.55 ± 0.01	0.65	3.98 ± 0.02	0.50
Cer1P	2	d18:1/18:1	0.26 ± 0.04	16.38	0.72 ± 0.01	2	1.03 ± 0.02	1.74	1.62 ± 0.03	1.76	4.29 ± 0.36	8.42

[a]Mixing ratio of each methylated lipids.

ion mode, supporting that methylation of PA and CL enhanced their detection during MS. This demonstrates that ionization interference from methylation products of PEs and intact PCs was not significant to suppress the ionization of the four lipid classes of interests, as all lipids that were identified from intact and nonmethylated PLs were identified from the ILM-based method as well. Especially, the identified number of CLs increased to 43 from methylated extracts while only 18 species were identified from the intact PL extracts. This is an outstanding improvement compared to the reported numbers of identified CLs (24 from PC-3 cell[37] and 28 from rat liver[38] using high-resolution LC−MS). The enhancement in CL detection is thought to be brought about by the enhanced ionization of methylated CL molecules due to the increase in their hydrophobicity. Moreover, the determination of four acyl chain locations in the intact CL, which was otherwise difficult, was achieved for each pair of acyl chains, i.e., (16:0,16:1), (18:1,18:1)-CL and (16:1,18:1),(16:0,18:1)-CL, post methylation. A series of CID spectra of methylated CL from the cell extract are illustrated in Figure S6 of the Supporting Information, showing that the molecular structures of each set of two acyl chains can be clearly distinguished from the MS^3 experiment of fragment ions ($[R_1CO_2CH_2(R_2CO_2)CHCH_2]^+$), which were readily produced with high intensities from MS^2 experiment of the ammonium adduct of methylated cardiolipin molecules. To the best of our knowledge, this is the first report demonstrating the identification of sets of acyl chain locations at each glycerol molecule of CL in positive ion mode. For validation of the ILM-based quantification, the measured D/H values were compared with those obtained from the conventional quantification methods in which both the intact PL extracts (with or without treatment of D-allose) were analyzed individually and the amount of each species was measured with the corrected peak area relative to that of the internal standard (IS) specific to each headgroup. Comparison of the two quantification methods was performed for 4 PGs, 4 PSs, 10 PAs, and 8 CLs containing no isomeric chain structures by Student's *t* test (Table S5) since ILM-based quantification relies on the total number of carbon and double bonds in acyl chains, whereas the conventional quantification method relies on individual isomeric molecules. The calculated *p*-values from the two methods were found to be larger than 0.05 for all the samples, except 18:1/18:1-PS, confirming that the ILM-based quantification method was not statistically different from the conventional method.

The results in Table S4 demonstrate that most PS, PA, and CL species were decreased whereas some PGs were increased upon the treatment with D-allose. Species exhibiting changes of more than 30% in the D/H ratio are marked in bold. The decrease in the amount of PS and PA could be attributed to the antiproliferative effect of D-allose on DU145 cells, which, in turn, may be a result of mitochondria-mediated apoptotic pathway.[39] Increase in the levels of PG with decreased trends in PA and CL could be explained by the fact that CL is synthesized from PG by the enzyme CL synthase in the presence of cytidine diphosphate diacylglycerol (CDP-diacylglycerol), which is produced from PA by PA cytidylyltransferase using cytidine triphosphate (CTP) as a precursor.[40] The significant decrease in the amount of PA (2−3-fold for all

DOI: 10.1021/acs.analchem.7b00297
Anal. Chem. 2017, 89, 4969−4977

19 PAs except 16:0-LPA) post D-allose treatment, therefore, may inhibit the conversion of PG into CL (Table S4).

CONCLUSIONS

In the present study, the capability of ILM-based quantification method was validated in the positive ion mode, using an optimized ionization modifier, 5 mM AF. This method improved the efficiency of ESI and increased the hydrophobicity of PLs, which resulted in longer retention times. The shifted retention times of H- and D-methylated lipids were nearly the same, which proved that PLs from a mixture of two different samples of interest can be analyzed at the same time without using internal standards. The efficiency of methylation was higher than 96% for most of the classes of PLs, except for LPI (~92.4%), under acidic conditions. A good linear relationship was observed between H- and D-methylated PLs, with error values less than 6.6%. The ILM-based quantification method was compared with the conventional method that utilizes internal standards from all classes of PLs and was found to be equally effective, based on the *p*-values from Student's *t* test, which were greater than 0.05 for all the classes of lipids except 18:1/18:1-PS. The study highlighted several advantages of the ILM-based method, such as the detection of additional PLs (8 PAs and 25 CLs) that were not detected from intact PL extracts, the improved analysis of CLs by increased detection capability of the methylated CLs, and the distinguishable determination of 4 acyl chains with location. As the CLs are specifically found in mitochondria, the ILM-based quantification method can be applied for the lipidomic assessment of mitochondrial-related diseases in particular. While the current method was not applied for PCs and PEs, utilization of C^{13} labeled TMSD would result in methylated PEs to have 3 Da larger *m/z* values than intact PCs having identical acyl chain structures since it was known that methylation of PE can be made as a combination of three methylation at primary amine or two methylation at primary amine with methylation at the phosphate group.[27]

ASSOCIATED CONTENT

Supporting Information

The Supporting Information is available free of charge on the ACS Publications website at DOI: 10.1021/acs.analchem.7b00297.

Materials and reagents; column preparation and nUPLC–ESI-MS/MS system configuration; additional chromatograms; table of average retention time and the difference in retention times between H- and D-methylated PL standards; types of precursor and quantifier ions of methylated PLs selected for SRM quantitation; influence of matrix effect; and quantification results (PDF)

AUTHOR INFORMATION

Corresponding Author

*Phone: (82) 2 2123 5634. Fax: (82) 2 364 7050. E-mail: mhmoon@yonsei.ac.kr.

ORCID

Myeong Hee Moon: 0000-0002-5454-2601

Author Contributions

The manuscript was written through contributions of all authors.

Notes

The authors declare no competing financial interest.

ACKNOWLEDGMENTS

This study was supported by the Grant NRF-2015R1A2A1A01004677 from the National Research Foundation (NRF) of Korea.

REFERENCES

(1) Brouwers, J. F.; Vernooij, E. A.; Tielens, A. G.; van Golde, L. M. *J. Lipid Res.* **1999**, *40*, 164–169.
(2) Wenk, M. R. *Nat. Rev. Drug Discovery* **2005**, *4*, 594–610.
(3) Kröger, J.; Zietemann, V.; Enzenbach, C.; Weikert, C.; Jansen, E. H.; Döring, F.; Joost, H. G.; Boeing, H.; Schulze, M. B. *Am. J. Clin. Nutr.* **2011**, *93*, 127–142.
(4) Grundy, S. M.; Cleeman, J. I.; Daniels, S. R.; Donato, K. A.; Eckel, R. H.; Franklin, B. A.; Gordon, D. J.; Krauss, R. M.; Savage, P. J.; Smith, S. C., Jr.; Spertus, J. A.; Costa, F. *Circulation* **2005**, *112*, 2735–2752.
(5) Meshkani, R.; Adeli, K. *Clin. Biochem.* **2009**, *42*, 1331–1346.
(6) Kiens, B. *Physiol. Rev.* **2006**, *86*, 205–243.
(7) Byeon, S. K.; Lee, J. Y.; Lee, J. S.; Moon, M. H. *J. Chromatogr. A* **2015**, *1381*, 132–139.
(8) Lee, J. C.; Kim, I. Y.; Son, Y.; Byeon, S. K.; Yoon, D. H.; Son, J. S.; Song, H. S.; Song, W.; Seong, J. K.; Moon, M. H. *Sci. Rep.* **2016**, *6*, 29617–29626.
(9) Isaac, G.; Bylund, D.; Månsson, J. E.; Markides, K. E.; Bergquist. *J. Neurosci. Methods* **2003**, *128*, 111–119.
(10) Taguchi, R.; Hayakawa, J.; Takeuchi, Y.; Ishida, M. *J. Mass Spectrom.* **2000**, *35*, 953–966.
(11) Cajka, T.; Fiehn, O. *TrAC, Trends Anal. Chem.* **2014**, *61*, 192–206.
(12) Kim, H.; Min, H. K.; Kong, G.; Moon, M. H. *Anal. Bioanal. Chem.* **2009**, *393*, 1649–1656.
(13) Min, H. K.; Kong, G.; Moon, M. H. *Anal. Bioanal. Chem.* **2010**, *396*, 1273–1280.
(14) Lee, J. Y.; Byeon, S. K.; Moon, M. H. *Anal. Chem.* **2015**, *87*, 1266–1273.
(15) Byeon, S. K.; Lee, J. Y.; Lee, J. S.; Moon, M. H. *J. Chromatogr. A* **2015**, *1381*, 132–139.
(16) Lee, S. T.; Lee, J. C.; Kim, J. W.; Cho, S. Y.; Seong, J. K.; Moon, M. H. *Sci. Rep.* **2016**, *6*, 36510–36520.
(17) Koivusalo, M.; Haimi, P.; Heikinheimo, L.; Kostiainen, R.; Somerharju, P. *J. Lipid Res.* **2001**, *42*, 663–672.
(18) Wang, M.; Wang, C.; Han, X. *Mass Spectrom. Rev.* **2016**, DOI: 10.1002/mas.21492.
(19) Ahn, E. J.; Kim, H.; Chung, B. C.; Moon, M. H. *J. Sep. Sci.* **2007**, *30*, 2598–2604.
(20) Berry, K. A. Z.; Murphy, R. C. *J. Lipid Res.* **2005**, *46*, 1038–1046.
(21) Zemski Berry, K. A.; Turner, W. W.; VanNieuwenhze, M. S.; Murphy, R. C. *Anal. Chem.* **2009**, *81*, 6633–6640.
(22) Nie, S.; Fhaner, C. J.; Liu, S.; Peake, D.; Kiyonami, R.; Huang, Y.; Reid, G. E. *Int. J. Mass Spectrom.* **2015**, *391*, 71–81.
(23) Wang, X.; Wei, F.; Xu, J. Q.; Lv, X.; Dong, X. Y.; Han, X.; Quek, S. Y.; Huang, F. H.; Chen, H. *Anal. Chim. Acta* **2016**, *902*, 142–153.
(24) Lee, J. W.; Nishiumi, S.; Yoshida, M.; Fukusaki, E.; Bamba, T. *J. Chromatogr. A* **2013**, *1279*, 98–107.
(25) Kim, S. H.; Song, H. E.; Kim, S. J.; Woo, D. C.; Chang, S.; Choi, W. G.; Kim, M. J.; Back, S. H.; Yoo, H. J. *J. Lipid Res.* **2017**, *58*, 469–478.
(26) Wasslen, K. V.; Canez, C. R.; Lee, H.; Manthorpe, J. M.; Smith, J. C. *Anal. Chem.* **2014**, *86*, 9523–9532.
(27) Canez, C. R.; Shields, S. W.; Bugno, M.; Wasslen, K.; Weinert, H.; Willmore, W. G.; Smith, J. C. *Anal. Chem.* **2016**, *88*, 6996–7004.
(28) Cai, T.; Shu, Q.; Hou, J.; Liu, P.; Niu, L.; Guo, X.; Liu, C. C.; Yang, F. *Anal. Chem.* **2015**, *87*, 513–521.

DOI: 10.1021/acs.analchem.7b00297
Anal. Chem. 2017, 89, 4969–4977

(29) Cai, T.; Shu, Q.; Liu, P.; Niu, L.; Guo, X.; Ding, X.; Xue, P.; Xie, Z.; Wang, J.; Zhu, N.; Wu, P.; Niu, L.; Yang, F. *J. Lipid Res.* **2016**, *57*, 388−397.
(30) Murata, A.; Sekiya, K.; Watanabe, Y.; Yamaguchi, F.; Hatano, N.; Izumori, K.; Tokuda, M. *J. Biosci. Bioeng.* **2003**, *96*, 89−91.
(31) Naha, N.; Lee, H. Y.; Jo, M. J.; Chung, B. C.; Kim, S. H.; Kim, M. O. *Apoptosis* **2008**, *13*, 1121−1134.
(32) Kagan, V. E.; Borisenko, G. G.; Tyurina, Y. Y.; Tyurin, V. A.; Jiang, J.; Potapovich, A. I.; Kini, V.; Amoscato, A. A.; Fujii, Y. *Free Radical Biol. Med.* **2004**, *37*, 1963−1985.
(33) Byeon, S. K.; Lee, J. Y.; Moon, M. H. *Analyst* **2012**, *137*, 451−458.
(34) Lim, S.; Byeon, S. K.; Lee, J. Y.; Moon, M. H. *J. Mass Spectrom.* **2012**, *47*, 1004−1014.
(35) Santa, T. *Biomed. Chromatogr.* **2011**, *25*, 1−10.
(36) Scheffler, I. E. *Mitochondrion* **2001**, *1*, 3−31.
(37) Sapandowski, A.; Stope, M.; Evert, K.; Evert, M.; Zimmermann, U.; Peter, D.; Päge, I.; Burchardt, M.; Schild, L. *Mol. Cell. Biochem.* **2015**, *410*, 175−185.
(38) Bird, S. S.; Marur, V. R.; Sniatynski, M. J.; Greenberg, H. K.; Kristal, B. S. *Anal. Chem.* **2011**, *83*, 940−949.
(39) Naha, N.; Lee, H. Y.; Jo, M. J.; Chung, B. C.; Kim, S. H.; Kim, M. O. *Apoptosis* **2008**, *13*, 1121−1134.
(40) McMillin, J. B.; Dowhan, W. *Biochim. Biophys. Acta, Mol. Cell Biol. Lipids* **2002**, *1585*, 97−107.

DOI: 10.1021/acs.analchem.7b00297
Anal. Chem. 2017, 89, 4969−4977